Volume 22, No 4 | International Journal of Radiation Research, October 2024

Logistic regression analysis of imaging characteristics of transvaginal ultrasonography for predicting severe endometriosis by r-ASRM classification via laparoscopy

Q. Su[1], H. Luo[2], J. Guo[1], H. Ning[2], Zh. Xu[2], Ch. Zhen[3], J. Chen[2], F. Wang[3], Q. Li[4], P. Wang[1*]

[1]Department of Ultrasonography, The Third Affiliated Hospital, Southern Medical University, Guangzhou, 510630, Guangdong, China
[2]Department of Ultrasound, Foshan Women and Children Hospital Affiliated to Guangdong Medical University, 528000, Guangdong, China
[3]Department of Ultrasound, The First People's Hospital of Foshan, Foshan,528000, Guangdong, China
[4]Department of Gynecology, Foshan Women and Children Hospital Affiliated to Guangdong Medical University, Foshan, 528000, Guangdong, China

► ***Original article***

Corresponding author:
Ping Wang, Ph.D.,
E-mail:
nysycskwp123@smu.edu.cn

Received: January 2023
Final revised: January 2024
Accepted: February 2024

Int. J. Radiat. Res., October 2024; 22(4): 991-998

DOI: 10.61186/ijrr.22.4.998

Keywords: *Endometriosis, laparoscope, regression analysis, ultrasonography.*

ABSTRACT

Background: To explore the relation between results of transvaginal ultrasonography and the revised American Society for Reproductive Medicine (r-ASRM) staging based on laparoscopy in patients with endometriosis (EMT) and to establish a prediction model for risk of severe endometriosis based on the imaging characteristics of transvaginal ultrasonography. ***Materials and Methods:*** A retrospective study was performed between April 2022 and May 2023 on women with EMT. The laparoscopic surgery results were used as the golden standard. Patients were divided into the minimal-to-moderate endometriosis (stage I-III) and severe endometriosis (stage IV) groups based on r-ASRM classification. The transvaginal ultrasonography imaging characteristics were extracted to establish a logistic regression model. ***Results:*** Among 200 patients with endometriosis, there were 78 cases of minimal-to-moderate endometriosis (stage I-III) and 122 cases of severe endometriosis (stage IV). Multivariate analysis showed that the maximum diameter of endometriomas in the right ovary, occurrence of unilateral or bilateral ovarian endometriomas, and degree of obliteration of the rectouterine pouch were independent predictors for the r-ASRM stage of endometriosis. The logistic regression model established using the above three variables had a sensitivity of 82.0%, a specificity of 93.6%, an accuracy of 86.5%, and an area under the curve of 0.933 (standard error 0.016, $P < 0.005$, 95% confidence interval: 0.901, 0.965). ***Conclusion:*** Based on laparoscopic visualization, the radiomic features of preoperative transvaginal ultrasonography in patients with endometriosis were correlated with the endometriotic stage. The established model using these characteristics accurately predicted the r-ASRM stage of endometriosis after laparoscopic surgery.

INTRODUCTION

Endometriosis (EMT) refers to the presence of active EMT tissues (glands and stroma) outside of the uterus [1], causing unbearable chronic pain and infertility. Approximately 30% ~ 50% of women with endometriosis struggle with infertility, and 25% ~ 50% of women with infertility also have endometriosis [2]. Laparoscopic surgery is the most common intervention for EMT [3]. Since 1996, the revised American Society for Reproductive Medicine (r-ASRM) classification system has been widely used worldwide for the staging of EMT lesions via laparoscopic visualization, categorizing EMT in the pelvic area into four stages: minimal (stage I), mild (stage II), moderate (Stage III), and severe (stage IV) EMT [4]. However, r-ASRM classification is done after laparoscopic surgery, which also indicates that the necessity of laparoscopic surgery should be effectively evaluated. Since the r-ASRM classification system does not include many affected organs and anatomical structures in the pelvic cavity, it has not been directly applied in preoperative examination [5]. The early diagnosis of EMT before treatment and accurate assessment after treatment is essential for the effective clinical management [6,7].

The diagnosis of EMT is challenged due to the heterogeneity of the disease, uncertainty in pathogenesis, asymptom, and complication with adenomyosis [8]. Currently, the diagnosis of EMT

[DOI: 10.61186/ijrr.22.4.998]

includes ultrasonography, magnetic resonance imaging (MRI), measurement of the serum cancer antigen 125 level, and laparoscopic surgery. Histological confirmation of ectopic endometrial tissue via laparoscopy remains the gold standard for the diagnosis of EMT, while the applicability is limited by the invasive procedure [6]. Transvaginal ultrasonography has the advantages as follows: (i) the accurate prediction of EMT severity by displaying the fine structure of organs and tissues in the pelvic cavity; (ii) the effective evaluation of the distribution and infiltration of deep infiltrating EMT (DIE) lesions in various parts of the pelvic cavity. Transvaginal ultrasonography has become the first-line approach for screening EMT [9,10]. Compared with MRI, transvaginal ultrasonography shows relatively higher specificity in the detection of deep infiltrating endometriosis [11]. Moreover, the transvaginal ultrasonography and MRI show no systemic difference in the EMT detection compared with the intraoperative measurement, and transvaginal ultrasonography is more recommended for the diagnostic examination due to its high availability, low cost and similar accuracy relative to MRI [12,13].

In the present study, we analyzed the correlation between the transvaginal ultrasonography imaging characteristics in EMT and r-ASRM classification after laparoscopic surgery to assess the surgical difficulty preoperatively, which might provide the theoretical basis and novel clues for the effective and accurate diagnosis and management of EMT.

MATERIALS AND METHODS

Research participants

We retrospectively analyzed the clinical data of 200 patients (aged 19-51 years) with DIE screened by transvaginal ultrasonography in Foshan Maternal and Child Health Hospital (Guangdong Province, China) from August 2021 to December 2022. All patients underwent laparoscopic surgery for treatment, and EMT was pathologically confirmed. The clinical data collected in this study included clinical symptoms and signs, surgical records, surgical staging, and pathological data. The laparoscopic surgery-based r-ASRM classification included four EMT stages: minimal (stage I), mild (stage II), moderate (stage III), and severe (stage IV). Laparoscopic surgery results were used as the gold standard. Patients were divided into two groups based on their r-ASRM stage: the minimal-to-moderate group (stage I-III) and the severe group (stage IV).

Research apparatus and methods

A Samsung WS80A Ultrasound Machine was used, with an intracavity probe frequency ranging from 5 to 9 Mega Hertz (MHz) and 9 to 12 MHz. An abdominal probe was used with a frequency ranging from 5 to 9 MHz.

Ultrasonography

The patient took the lithotomy position, after which their vagina, uterus, anterior pelvic cavity, posterior pelvic cavity, and specific tender points were successively scanned through the vagina. The collected cases were independently reviewed by two blinded radiologists (each with more than 5 years of ultrasonography experience). They analyzed the images following the consensus issued by the International Deep EMT Analysis Group (referred to as consensus) [14] and discrepancies were resolved by discussion between the two radiologists. The location, number, size and imaging manifestation of EMT lesions were recorded in a standardized report.

Laparoscopic surgery

Experienced surgeons operated on all patients. The pelvic and abdominal cavity and the EMT lesions were assessed. After removing the connective tissues to expose the affected areas completely, the lesions, including the adjacent tissue up to 0.5 centimeters from the outer edge, were excised. The appearance of the abdominal adhesions, the uterus, the uterosacral ligament, fallopian tubes, the rectum and the presence of EMT lesions were recorded. A postoperative r-ASRM scoring table was completed to classify the EMT as minimal (stage I), mild (stage II), moderate (stage III), or severe (stage IV).

Statistical analysis

The SPSS23.0 software package (IBM, Armonk, NY, USA) was used for the statistical analysis of the data. Normally distributed data were compared using the t-test and presented as the mean ± standard deviation. Non-normally distributed data were compared using the rank sum test and are presented as median (M) and interquartile range (P25, P75). Count data were compared using the chi-square test and were presented as frequency (n) and percentage (%). Multivariate analysis was carried out by binary logistic regression. $P < 0.05$ was considered significant.

RESULTS

Results of r-ASRM classification of endometriotic lesions

Among 200 patients with EMT, according to the r-ASRM classification, there were 78 cases of minimal-to-moderate EMT (stage I – III) and 122 cases of severe EMT (stage IV). Table 1 shows the clinical characteristics and affected sites of all patients in this study. The ultrasound imaging features of different lesions are shown in figures 1-4. As shown in figure 1, the ovaries of this patient were partly joined

[DOI: 10.61186/ijrr.22.4.998]

together, termed as "kissing ovaries" sign, and bilateral ovarian endometriotic cysts were also observed. Figure 2 showed that this DIE patient presented nodules infiltrating the right uterosacral ligament. Figure 3 exhibited that the lesion of this DIE patient was located at the intestines with blur and spiculate boundary as the "Indian headdress". Figure 4 showed the rectouterine pouch obliteration. The lesion adheres to surrounding tissues, and the rectum slid against the uterine wall, termed as uterine sliding sign. Bilateral uterosacral ligament and intestinal DIE under the hysteroscopic are shown in figures 5 and 6. As shown in figure 5, the observation under a hysteroscope identified the infiltrating nodules at bilateral uterosacral ligament of the DIE patient. Figure 6 indicated that the patient presented endometriotic cyst in the right ovarian and the intestinal lesion under a hysteroscope.

Table 1. Baseline characteristics of patients.

	I-III **(n=78)**	IV **(n=122)**	t/c^2	P
Age (years)	33.62±5.87	34.33±7.61	0.742	0.459
Age of menarche	12.87±1.21	13.01±1.08	0.832	0.407
marital status			0.619	0.431
Married (n)	59	98		
Unmarried (n)	19	24		
Pregnancy history			1.518	0.218
Yes	24	48		
No	54	74		
BMI (kg/m^2)	23.8±4.2	24.1±3.9	0.507	0.613
Infertility	22	41	0.643	0.423
Uterine adenomyosis				
No	61	69	9.801	0.002
Yes	17	53		
Uterine size				
No	68	89	5.707	0.017
Yes	10	33		
Ovarian lesions				
No	9	3	57.199	0.000
Unilateral involvement	65	49		
Bilateral involvement	4	70		
Ovarian dislocation movement				
Exist	25	11	38.359	0.000
One-sided disappearance	34	28		
Bilateral disappearance	19	83		
Rectal notch with or without occlusion				
No	42	5	82.715	0.000
One-sided occlusion	32	51		
Bilateral occlusion	4	66		
Douglas' lieaments DIE				
No	41	33	26.803	0.000
Hemi	30	38		
Bilateral	7	51		
Rectal / sigmoid colon DIE				
No	67	77	12.250	0.000
Yes	11	45		
DIE of the serosal layer of the posterior uterine wall				
No	71	86	11.887	0.001
Yes	7	36		
Anterior vaginal fornix with tenderness				
No	77	120	0.041	0.839
Yes	1	2		
The posterior vaginal fornix was tender				
No	61	100	0.429	0.512
Yes	17	22		
The left appendage area was tender				
No	53	80	0.120	0.729
Yes	25	42		
The right accessory area was tender				
No	60	82	2.179	0.140
Yes	18	40		
The left sacral ligament was tender				
No	65	92	1.770	0.183
Yes	13	30		
The right sacral ligament was tender				
No	74	97	9.059	0.003
Yes	4	25		

BMI: body mass index; DIE: deep infiltrating endometriosis.

[DOI: 10.61186/ijrr.22.4.998]

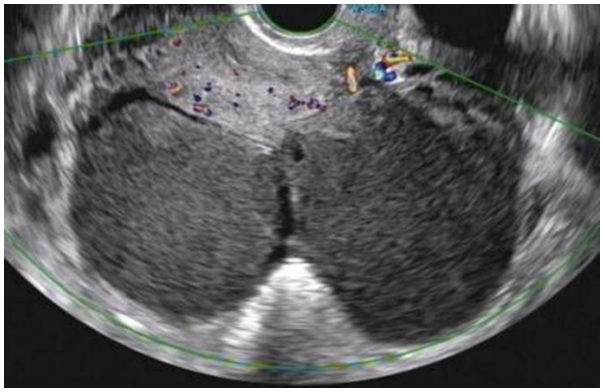

Figure 1. A representative transvaginal ultrasonography image showed the kissing ovaries sign with bilateral ovarian endometriotic cysts.

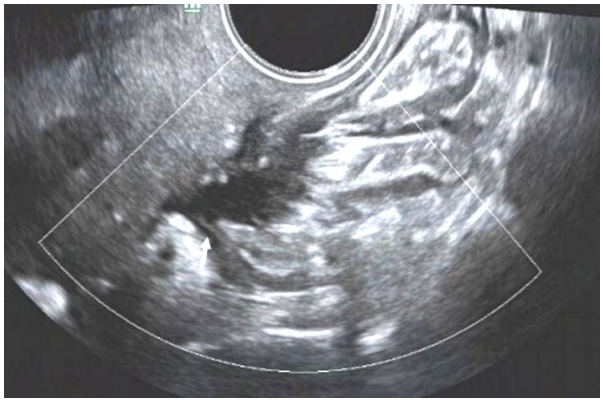

Figure 3. A representative transvaginal ultrasonography image showed the Indian headdress sign of intestinal DIE.

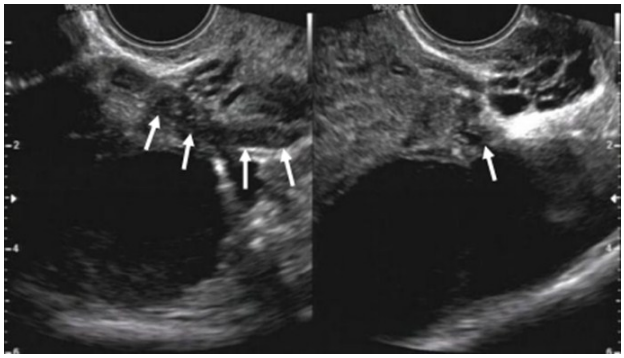

Figure 2. Representative transvaginal ultrasonography images showed right uterosacral ligament deep infiltrating endometriosis (DIE).

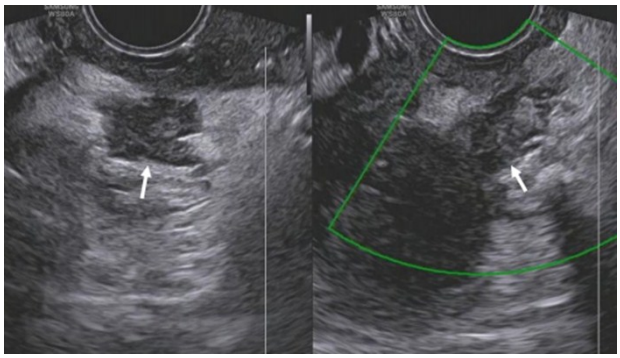

Figure 4. Representative transvaginal ultrasonography images of a DIE patient with the obliteration of the rectouterine pouch. The lesion adheres to surrounding tissues, and the presented uterine sliding sign indicated the obliteration of the rectouterine pouch.

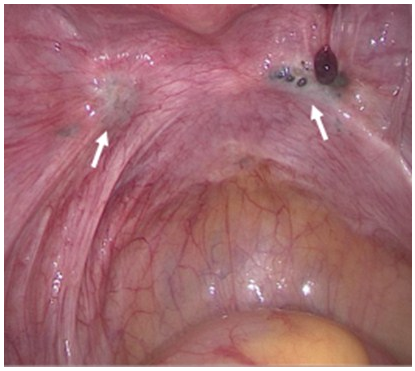

Figure 5. Bilateral uterosacral ligament in a DIE patient under the hysteroscope.

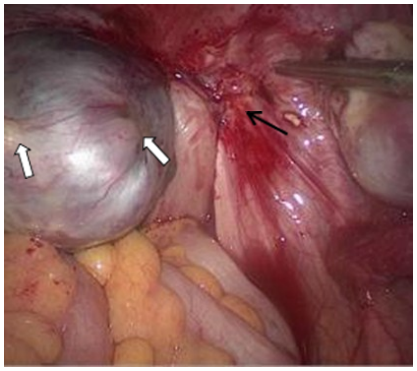

Figure 6. Right ovarian endometriotic cyst ("white arrow" as shown) and intestinal DIE ("black arrow" as shown) under the hysteroscope.

Univariate analysis of the diagnostic efficacy of imaging characteristics

Based on univariate analysis, we analyzed a total of 49 variables, including age, the presence of adenomyosis, uterine size, ovarian EMT, the disappearance of bilateral ovarian malposition and motion, the degree of obliteration of the rectouterine pouch, DIE size and DIE distribution in the fallopian tube, kidney, renal ureters, urethra, bladder, bladder uterine peritoneal reflection, rectouterine pouch, rectovaginal septum, rectum/ sigmoid colon, serosa of the posterior uterine wall and posterior fornix of the vagina. The results of the univariate analysis showed that the r-ASRM stage of EMT lesions was correlated with the presence of adenomyosis, uterine enlargement, the occurrence of unilateral or bilateral ovarian endometrioma, the disappearance of unilateral or bilateral ovarian malposition and motion, the degree of the rectouterine pouch obliteration, the degree of uterosacral ligament involvement, involvement of the rectum/ sigmoid colon, involvement of the serosa of the posterior uterine wall, the presence of tenderness in the right uterosacral ligament, the maximum diameters of chocolate cysts in the left and right ovaries, maximum diameters of DIE lesions located in the left and right uterosacral ligaments, the maximum diameter and infiltration depth of intestinal DIE lesions, and the maximum diameter and infiltration depth of EMT lesions in the serosa of the posterior uterine wall (all $P < 0.05$, see table 2 for details).

[DOI: 10.61186/ijrr.22.4.998]

Multivariate analysis of the diagnostic value of imaging characteristics

Multivariate binary logistic regression analysis was conducted with r-ASRM Stage IV as the dependent variable. Our results showed that the size of the right ovarian endometrioma, the occurrence of unilateral or bilateral ovarian endometrioma, and the degree of obliteration of the rectouterine pouch were independent predictors for r-ASRM stage in EMT patients (P < 0.05, table 3). The following logistic regression equation was established: −7.901 + (0.031 × maximum diameter [long diameter, unit: mm] of right ovarian endometrioma) + (2.437 × unilateral or bilateral ovarian endometrioma occurrence) + (2.888 × degree of rectouterine pouch obliteration). Table 4 showed the assigned values for regression analysis, with an intercept of – 0.337.

The receiver operating characteristic (ROC) curve was prepared using the predicted values. The predictive ability of this model was evaluated using the area under the ROC curve (figure 7). The logistic regression model established based on the imaging characteristics of ultrasonography showed a sensitivity of 82.0%, a specificity of 93.6%, an accuracy of 86.5%, and an area under the curve of 0.933 (standard error 0.016, P < 0.05, 95% confidence interval: 0.901, 0.965).

Table 2. Univariate analysis of the diagnostic efficacy of imaging characteristics.

	I-III (n=78)	IV (n=122)	T/Z	P
Age	33.62±5.87	34.33±7.61	-0.744	0.458
Long diameter of left ovary	0.00 (0.00, 57.25)	36.00 (0.00, 70.00)	-2.538	0.011
Long diameter of right ovary	0.00 (0.00, 56.25)	48.50 (21.75, 72.25)	-4.698	0.000
DIE diameter of left uterosacral ligament	0.00 (0.00, 10.00)	7.50 (0.00, 13.00)	-2.434	0.015
DIE diameter of right uterosacral ligament	0.00 (0.00, 0.00)	9.00 (0.00, 15.00)	-5.461	0.000
Intestinal DIE length	0.00 (0.00, 0.00)	0.00 (0.00, 16.00)	-3.514	0.000
Gut DIE depth	0.00 (0.00, 0.00)	0.00 (0.00, 6.00)	-3.536	0.000
The DIE length of the uterine serosal layer	0.00 (0.00, 0.00)	0.00 (0.00, 10.00)	-3.436	0.001
The DIE depth of the uterine serosal layer	0.00 (0.00, 0.00)	0.00 (0.00, 4.00)	-3.412	0.001

DIE: deep infiltrating endometriosis.

Table 3. Binary logistic regression results.

	B	standard error	Wald	conspicuousness	OR	The 95% confidence intervals of the OR	
						lower limit	superior limit
Left of left size (long diameter in mm)	0.022	0.012	3.742	0.053	1.023	1.000	1.046
Right sac size (long diameter in mm)	0.031	0.013	5.978	0.014	1.032	1.006	1.058
Left uterosacral ligament DIE diameter (in mm)	0.028	0.059	0.219	0.640	1.028	0.916	1.154
Right uterosacral ligament DIE diameter (in mm)	0.065	0.065	0.987	0.320	1.067	0.939	1.212
DIE length (in mm)	0.052	0.067	0.615	0.433	1.054	0.925	1.201
DIE depth (in mm)	0.004	0.139	0.001	0.979	1.004	0.764	1.318
DIE of uterine serous layer (in mm)	0.169	0.126	1.801	0.180	1.184	0.925	1.515
DIE depth of uterine serosa layer (in mm)	-0.296	0.286	1.071	0.301	0.744	0.425	1.303
Uterine adenomyosis	-.593	0.655	0.820	0.365	0.553	0.153	1.994
uterine size	1.055	0.825	1.635	0.201	2.871	0.570	14.456
Ovarian lesions	2.437	0.770	10.025	0.002	11.440	2.531	51.714
Ovarian dislocation movement	-.385	0.466	0.682	0.409	0.680	0.273	1.697
Rectal notch with or without occlusion	2.888	0.585	24.407	0.000	17.951	5.709	56.446
Douglas' lieaments DIE	0.420	0.739	0.322	0.570	1.521	0.357	6.476
A DIE of the rectosigmoid colon	-0.976	1.410	0.480	0.489	0.377	0.024	5.968
DIE of the serosal layer of the posterior uterine wall	0.201	1.915	0.011	0.916	1.222	0.029	52.103
The right sacral ligament was tender	0.347	0.927	0.140	0.708	1.415	0.230	8.709

OR: odds ratio; DIE: deep infiltrating endometriosis.

Table 4. The area below the curve.

Test the outcome variable	AUC	standard error[a]	The asymptotic significance[b]	Asymptotic 95% confidence interval	
				lower limit	superior limit
Right sac size (long diameter in mm)	0.694	0.039	0.000	0.618	0.770
Ovarian lesions	0.774	0.033	0.000	0.710	0.838
Rectal notch with or without occlusion	0.849	0.028	0.000	0.795	0.903
prediction model	0.933	0.016	0.000	0.901	0.965

AUC: area under the curve.

[DOI: 10.61186/ijrr.22.4.998]

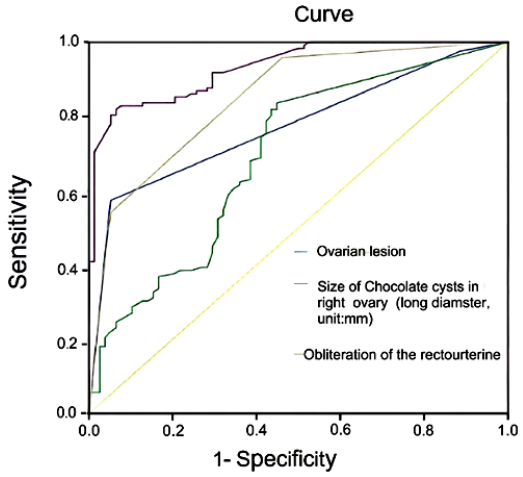

Figure 7. Receiver operating characteristic (ROC) curve evaluates the predictive ability of the logistic regression model established in this study for severe endometriosis. The curve shows an area under the curve of 0.933, a standard error of 0.016, P < 0.05 and a 95% confidence interval of (0.901, 0.965).

DISCUSSION

EMT-induced chronic pelvic pain and infertility seriously affect the quality of life of childbearing women globally. The most important role of r-ASRM classification is to predict the postoperative capabilities of natural pregnancy in patients with EMT and provide treatment options [15]. Laparoscopic resection of EMT lesions is the most common treatment method for EMT. However, the procedure is challenging, highly dependent on the clinical experience and surgical skills of surgeons and may trigger postoperative complications/ trauma. Thus, physicians are suggested to consider the preoperative imaging results to provide individualized treatment plans. With the development of high-frequency endo-cavity probes, more imaging details are obtained with pelvic ultrasound information for the diagnosis of EMT.

Previous studies have indicated that the adenomyosis is associated with endometriosis, especially the deep infiltrating lesions, and the severity of EMT was evaluated based on ASRM on preoperative transvaginal ultrasonography, and the results of transvaginal ultrasonography are closely correlated with those of the laparoscopic examination [16,17]. Moreover, adenomyosis, right endometrioma, right endometrioma ≥ 5 cm are regarded as independent risk factors for EMT [18]. A previous work also revealed that the transvaginal ultrasound sliding sign shows high sensitivity in the prediction of pouch of Douglas obliteration [19]. In the present study, we retrospectively analyzed the clinical data and ultrasonography imaging characteristics of EMT patients with confirmed r-ASRM stages after laparoscopic surgery. Our results showed that patients with adenomyosis and uterine enlargement showed severe EMT and a high risk of involvement of bilateral ovaries, bilateral uterosacral ligaments, the rectum/sigmoid colon, and the serosa of the posterior uterine wall (all P < 0.05), resulting in the disappearance of bilateral ovarian malposition and motion, complete obliteration of the rectouterine pouch, and tenderness in the right uterosacral ligament. Three independent predictors were screened out after univariate analysis, including the maximum diameter of the right ovarian endometrioma, the degree of obliteration of the rectouterine pouch, and unilateral or bilateral ovarian involvement (table 2) and the results are in line with the previous findings.

The classical theory of EMT pathogenesis is retrograde menstruation, in which endometrial, epithelial and stromal cells in the blood flow back into the pelvic cavity instead of the vagina, stimulating the proliferation of connective tissue or smooth muscle tissue to form lesions [20,21]. Also, anatomical and hormonal factors are considered to affect left lateral predisposition to EMT. For example, the presence of a sigmoid colon reduces the blood flow to the left side of the pelvic cavity, which may delay the clearance of endometrial cells through tubal reflux during menstruation, supporting the retrograde menstruation theory [22-24]. In the present study, the maximum diameter of the endometrioma in the right but not the left ovary had predictive power (table 3), which was consistent with the findings reported by Ulukus *et al*. that the incidence of ovarian endometrioma on the right side was higher than that on the left side in patients with severe EMT [25]. In the r-ASRM classification, the degree of adhesions on the ovaries greatly contributes to the r-ASRM score. However, ovarian malposition and motion had no independent predictive value in our study. This may be related to the influence of subjective factors, such as the imaging methods and the operator's judgment.

A multicenter study reveals that the transvaginal ultrasound is of high accuracy in the prediction of ASRM staging for EMT [26]. A recent study by Yang *et al*. have established a preoperative prediction model for the evaluation of risk factors related to severe EMT, with good diagnostic performance (AUC = 0.846) [27]. In the present study, we combined multiple imaging characteristics of ultrasonography and clinical-related factors to establish a model for predicting severe EMT (r-ASRM classification stage IV) via laparoscopic visualization through multivariate logistic regression analysis. The established model had a sensitivity of 82.0%, a specificity of 93.6%, an accuracy of 86.5%, and an area under the curve of 0.933 (standard error 0.016, P < 0.05, 95% confidence interval: 0.901, 0.965) in predicting severe EMT (table 4, figure 7). The predictive variables were all easy-to-obtain features that did not require invasive examinations.

[DOI: 10.61186/ijrr.22.4.998]

Our established model was simple, practical and easy to operate, with good performance relative to the previous models and could be applied in a real-time, fast, and repetitive manner in clinical practice.

In the era of precision medicine, a single indicator can no longer fulfill individualized treatment needs. It is necessary to comprehensively analyze the available information and screen out the risk factors to improve diagnostic accuracy. The prediction model established in this study is an easy-to-use tool with clinical value. The risk of severe EMT in each patient was determined using a simple equation, facilitating individualized treatment and assisting physicians in accurately determining each patient's disease severity and surgical difficulties.

Nevertheless, this study has some limitations. Elastography and contrast-enhanced ultrasonography have rapidly developed in recent years. Diagnostic ultrasound is no longer limited to simple grayscale and color Doppler imaging. Moreover, MRI has a certain value in the diagnosis and preoperative staging of EMT [28]. These factors were not included in this study. Follow-up research with larger samples should be conducted to further establish a prediction model in combination with multimodal imaging indicators to verify the accuracy and practicability of our model.

CONCLUSION

Transvaginal ultrasonography is valuable for EMT staging. The regression model established in this study using ultrasonic imaging characteristics effectively predicted the r-ASRM stage of EMT lesions, providing a basis for the diagnosis and treatment of EMT, assisting surgeons in predicting the degree of surgical risk before surgery accurately and improving individualized surgical treatment.

ACKNOWLEDGMENT

Not applicable.

Funding: This article is one of the achievements of the medical research project "Application of Endoscopic Ultrasound Elastic Imaging Technology Combined with Color Doppler in the Diagnosis of Deep Localized Endometriosis of the Pelvic Cavity" by the Foshan Municipal Health Bureau (project approval number 20210394).

Conflict of interests: All authors declared no conflicts of interest.

Data availability statements: The data that support the findings of this study are available on request from the corresponding author upon reasonable request.

Ethical consideration: Not applicable.

Author contribution: Q.S.: Conceptualization, data analysis, original draft; H.L., J.G.: H.N.: data collection, data analysis, reviewing and editing; Z.X., C.Z., J.C.: data collection, data analysis, reviewing; P.W.: Conceptualization, Supervision, reviewing and editing. All authors have read and approved the final version of the manuscript.

REFERENCES

1. Shafrir AL, Farland LV, Shah DK, *et al.* (2018) Risk for and consequences of endometriosis: A critical epidemiologic review. *Best Pract Res Clin Obstet Gynaecol*, ***51:*** *1-15.*
2. Evans MB and Decherney AH (2017) Fertility and endometriosis. *Clin Obstet Gynecol*, ***60(3):*** *497-502.*
3. Bafort C, Beebeejaun Y, Tomassetti C, *et al.* (2020) Laparoscopic surgery for endometriosis. *Cochrane Database Syst Rev*, ***10(10):*** *Cd011031.*
4. Johnson NP, Hummelshoj L, Adamson GD, *et al.* (2017) World endometriosis society consensus on the classification of endometriosis. *Hum Reprod*, ***32(2):*** *315-324.*
5. Tomassetti C, Bafort C, Vanhie A, *et al.* (2021) Estimation of the endometriosis fertility Index prior to operative laparoscopy. *Hum Reprod*, ***36(3):*** *636-646.*
6. Kido A, Himoto Y, Moribata Y, *et al.* (2022) MRI in the diagnosis of endometriosis and related diseases. *Korean Journal of Radiology*, ***23(4):*** *426-445.*
7. Bazot M and Daraï E (2017) Diagnosis of deep endometriosis: Clinical examination, ultrasonography, magnetic resonance imaging and other techniques. *Fertility and Sterility*, ***108(6):*** *886-894.*
8. Chapron C, Marcellin L, Borghese B, *et al.* (2019) Rethinking mechanisms, diagnosis and management of endometriosis. *Nature Reviews Endocrinology*, ***15(11):*** *666-682.*
9. Deslandes A, Parange N, Childs JT, *et al.* (2020) Current status of transvaginal ultrasound accuracy in the diagnosis of deep infiltrating endometriosis before surgery: A systematic review of the literature. *J Ultrasound Med*, ***39(8):*** *1477-1490.*
10. Guerriero S and Ajossa S (2020) Transvaginal ultrasonography in superficial endometriosis. *Aust N Z J Obstet Gynaecol*, ***60(3):*** *E5.*
11. Guerriero S, Saba L, Pascual MA, *et al.* (2018) Transvaginal ultrasound vs magnetic resonance imaging for diagnosing deep infiltrating endometriosis: Systematic review and meta-analysis. *Ultrasound in Obstetrics & Gynecology: The Official Journal of the International Society of Ultrasound in Obstetrics and Gynecology*, ***51(5):*** *586-595.*
12. Aas-Eng MK, Young VS, Dormagen JB, *et al.* (2023) Lesion-to-anal-verge distance in rectosigmoid endometriosis on transvaginal sonography vs magnetic resonance imaging: Prospective study. *Ultrasound in Obstetrics and Gynecology: The Official Journal of the International Society of Ultrasound in Obstetrics and Gynecology*, ***61(2):*** *243-250.*
13. Lee MS, Kim MD, Lee M, *et al.* (2012) Contrast-enhanced MR angiography of uterine arteries for the prediction of ovarian artery embolization in 349 patients. *Journal of Vascular and Interventional Radiology: JVIR*, ***23(9):*** *1174-1179.*
14. Indrielle-Kelly T, Frühauf F, Fanta M, *et al.* (2020) Application of international deep endometriosis analysis (IDEA) group consensus in preoperative ultrasound and magnetic resonance imaging of deep pelvic endometriosis. *Ultrasound Obstet Gynecol*, ***56(1):*** *115-116.*
15. Keckstein J, Oppelt P, Hudelist G (2022) Classification and clinical staging of endometriosis. In: Oral E, editor. Endometriosis and adenomyosis: Global perspectives across the lifespan. *Cham: Springer International Publishing*, *93-108*.
16. Chapron C, Tosti C, Marcellin L, *et al.* (2017) Relationship between the magnetic resonance imaging appearance of adenomyosis and endometriosis phenotypes. *Human Reproduction*, ***32(7):*** *1393-1401.*
17. Holland TK, Cutner A, Saridogan E, *et al.* (2013) Ultrasound mapping of pelvic endometriosis: Does the location and number of lesions affect the diagnostic accuracy? A multicentre diagnostic accuracy study. *BMC Women's Health*, ***13:*** *43.*
18. Mabrouk M, Raimondo D, Mastronardi M, *et al.* (2020) Endometriosis of the appendix: When to predict and how to manage-A multi-

[DOI: 10.61186/ijrr.22.4.998]

variate analysis of 1935 endometriosis cases. *Journal of Minimally Invasive Gynecology*, ***27(1):*** *100-106.*
19. Arion K, Aksoy T, Allaire C*, et al.* (2019) Prediction of pouch of douglas obliteration: Point-of-care ultrasound versus pelvic examination. *Journal of Minimally Invasive Gynecology*, ***26(5):*** *928-934.*
20. Borghese B, Santulli P, Marcellin L*, et al.* (2018) [Definition, description, clinicopathological features, pathogenesis and natural history of endometriosis: CNGOF-HAS Endometriosis Guidelines]. *Gynecol Obstet Fertil Senol*, ***46(3):*** *156-167.*
21. Koninckx PR, Fernandes R, Ussia A*, et al.* (2021) Pathogenesis based diagnosis and treatment of endometriosis. *Front Endocrinol (Lausanne)*, ***12:*** *745548.*
22. Vercellini P, Aimi G, De Giorgi O*, et al.* (1998) Is cystic ovarian endometriosis an asymmetric disease? *Br J Obstet Gynaecol*, ***105 (9):*** *1018-1021.*
23. Al-Fozan H and Tulandi T (2003) Left lateral predisposition of endometriosis and endometrioma. *Obstet Gynecol*, ***101(1):*** *164-166.*
24. Sznurkowski JJ and Emerich J (2008) Endometriomas are more frequent on the left side. *Acta Obstet Gynecol Scand*, ***87(1):*** *104-106.*
25. Ulukus M, Yeniel A, Ergenoglu AM*, et al.* (2012) Right endometrioma is related with more extensive obliteration of the Douglas pouch. *Arch Gynecol Obstet*, ***285(5):*** *1483-1486.*
26. Leonardi M, Espada M, Choi S*, et al.* (2020) Transvaginal ultrasound can accurately predict the american society of reproductive medicine stage of endometriosis assigned at laparoscopy. *Journal of Minimally Invasive Gynecology*, ***27(7):*** *1581-7. e1.*
27. Yang Y, Li J, Chen H*, et al.* (2022) Assessment of risk factors associated with severe endometriosis and establishment of preoperative prediction model. *Diagnostics (Basel, Switzerland)*, ***12(10)****.*
28. Bazot M, Kermarrec E, Bendifallah S*, et al.* (2021) MRI of intestinal endometriosis. *Best Pract Res Clin Obstet Gynaecol*, ***71:*** *51-63.*

[DOI: 10.61186/ijrr.22.4.998]